

# Invariant Amplitudes, Unpolarized Cross Sections, Polarization Observables in Charged-Current Elastic Neutrino-Nucleon Scattering

PIKIMO-15, Indiana University

**Kaushik Borah**

with M. Betancourt, R. J. Hill, T. R. Junk, O. Tomalak

[arXiv:2311.XXXXX](https://arxiv.org/abs/2311.XXXXX)

University of Kentucky

November 11, 2023



# Goal of the talk

- ▶ We present a general decomposition of (anti)neutrino-nucleon charged-current elastic scattering amplitudes.
- ▶ We evaluate the expressions for the unpolarized cross section and single-spin asymmetries in terms of these invariant amplitudes.
- ▶ We plot the numerical results for all observables as a function of  $Q^2$  at relevant fixed neutrino energies with tree-level nucleon form factors.
- ▶ We explore the impact of both unpolarized cross-section and polarized observables on constraining the amplitudes.

# Outline

## Theoretical Formulation

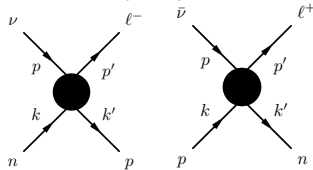
- Invariant Amplitudes
- Unpolarized Cross Section
- Polarization Observables

## Numerical Results

- Unpolarized Cross Section
- Polarization Observables

## Conclusion

# Amplitude decomposition for elastic (anti)neutrino-nucleon scattering



- ▶ In the  $m_\ell = 0$  limit, the matrix element of the charged-current elastic process can be given by,

$$T_{\nu_\ell n \rightarrow \ell^- p}^{m_\ell=0} = \sqrt{2}G_F V_{ud} \bar{\ell}^- \gamma^\mu P_L \nu_\ell \bar{p} \left( \gamma_\mu (\mathbf{g}_M + f_A \gamma_5) - (f_2 + f_A^3 \gamma_5) \frac{K_\mu}{M} \right) n$$

$$T_{\bar{\nu}_\ell p \rightarrow \ell^+ n}^{m_\ell=0} = \sqrt{2}G_F V_{ud}^* \bar{\nu}_\ell \gamma^\mu P_L \ell^+ \bar{n} \left( \gamma_\mu (\bar{\mathbf{g}}_M + \bar{f}_A \gamma_5) - (\bar{f}_2 - \bar{f}_A^3 \gamma_5) \frac{K_\mu}{M} \right) p$$

where,  $K_\mu = (k_\mu + k'_\mu)/2$ , the averaged nucleon momentum.

- ▶ For  $m_\ell \neq 0$ , the matrix element for charged currents contains four more invariant amplitudes,

$$T_{\nu_\ell n \rightarrow \ell^- p} = T_{\nu_\ell n \rightarrow \ell^- p}^{m_\ell=0} - \sqrt{2}G_F V_{ud} \frac{m_\ell}{M} \bar{\ell}^- P_L \nu_\ell \bar{p} \left( f_{P5} + f_P \gamma_5 - \frac{f_3 \not{P}}{4M} \gamma_5 \right) n$$

$$+ \sqrt{2}G_F V_{ud} \frac{m_\ell}{M} \frac{f_T}{4} \bar{\ell}^- \sigma^{\mu\nu} P_L \nu_\ell \bar{p} \sigma_{\mu\nu} n$$

$$T_{\bar{\nu}_\ell p \rightarrow \ell^+ n} = T_{\bar{\nu}_\ell p \rightarrow \ell^+ n}^{m_\ell=0} - \sqrt{2}G_F V_{ud}^* \frac{m_\ell}{M} \bar{\nu}_\ell P_R \ell^+ \bar{n} \left( \bar{f}_{P5} + \bar{f}_P \gamma_5 - \frac{\bar{f}_3 \not{P}}{4M} \gamma_5 \right) p$$

$$+ \sqrt{2}G_F V_{ud}^* \frac{m_\ell}{M} \frac{\bar{f}_T}{4} \bar{\nu}_\ell \sigma^{\mu\nu} P_R \ell^+ \bar{n} \sigma_{\mu\nu} p$$

where,  $P_\mu = (p_\mu + p'_\mu)/2$ , the averaged lepton momentum.

# Unpolarized Cross Section

- ▶ The charged-current elastic cross section, in the laboratory frame, is expressed in terms of invariant amplitudes as,

$$\frac{d\sigma}{dQ^2}(E_\nu, Q^2) = \frac{G_F^2 |V_{ud}|^2 M^2}{2\pi E_\nu^2} \left[ (\tau + r^2) A(\nu, Q^2) - \frac{\nu}{M^2} B(\nu, Q^2) + \frac{\nu^2}{M^4} \frac{C(\nu, Q^2)}{1 + \tau} \right]$$

- ▶ The quantities  $A$ ,  $B$ , and  $C$  are given by,

$$\begin{aligned} A &= \tau |g_M|^2 - |g_E|^2 + (1 + \tau) |f_A|^2 - r^2 \left( |g_M|^2 + |f_A + 2f_P|^2 - 4(1 + \tau) \left( |f_P|^2 + |f_{P5}|^2 \right) \right) \\ &\quad - \tau(1 + \tau) |f_A^3|^2 - 2r^2 \Re \left[ \left( g_E + 2g_M + (1 + \tau) f_A^3 \right) f_T^* \right] - \eta r^2 \left( 1 + \tau + r^2 \right) \Re \left[ f_A f_3^* \right] \\ &\quad + \frac{r^2}{4} \left( \nu^2 + 1 + \tau - \left( 1 + \tau + r^2 \right)^2 \right) |f_3|^2 - 2\eta r^4 \Re \left[ f_P f_3^* \right] - r^2 \left( 1 + 2r^2 \right) |f_T|^2, \end{aligned}$$

$$\begin{aligned} B &= \Re \left[ 4\eta \tau f_A^* g_M + 2\eta r^2 \left( f_A - 2\tau f_P \right)^* f_A^3 + 4r^2 g_E f_{P5}^* - 2\eta r^2 \left( 3f_A - 2\tau \left( f_P - \eta f_{P5} \right) \right) f_T^* \right. \\ &\quad \left. + r^4 \left( f_A^3 - f_T \right) f_3^* \right], \end{aligned}$$

$$C = \tau |g_M|^2 + |g_E|^2 + (1 + \tau) |f_A|^2 + \tau(1 + \tau) |f_A^3|^2 + 2r^2 (1 + \tau) |f_T|^2 + \eta r^2 (1 + \tau) \Re \left[ f_A f_3^* \right],$$

where,  $\eta = \pm 1$  for neutrino/antineutrino scattering.

# Single Spin Asymmetries

- ▶ The single-spin asymmetry is determined as the difference of the cross section  $\sigma(S)$  with a definite spin four-vector  $S$  of one initial- or final-state particle and the cross section with an opposite spin direction  $\sigma(-S)$  normalized to the unpolarized cross section as given by,

$$T, R, L = \frac{d\sigma(S) - d\sigma(-S)}{d\sigma(S) + d\sigma(-S)},$$

where we denote target, recoil, and lepton asymmetries as  $T$ ,  $R$ , and  $L$ .

- ▶ We can express  $T$ ,  $R$ , and  $L$  in terms of new structure-dependent functions as follows,

$$T, R, L = \frac{(\tau + r^2) A^{T,R,L}(\nu, Q^2) - \nu B^{T,R,L}(\nu, Q^2) + \frac{\nu^2}{1+\tau} C^{T,R,L}(\nu, Q^2)}{(\tau + r^2) A(\nu, Q^2) - \nu B(\nu, Q^2) + \frac{\nu^2}{1+\tau} C(\nu, Q^2)}$$

- ▶ We explore 3 special cases for each of  $T$ ,  $R$ , and  $L$ .
- ▶ For example, in the case of  $T$ ,
  - ▶  $T_t$  : target polarization is transverse to the beam direction with the spin vector in the scattering plane
  - ▶  $T_1$  : target polarization is along the beam direction
  - ▶  $T_\perp$  : target polarization is transverse to the scattering plane

# Single Spin Asymmetries

► For example, in the case of T,

$$\begin{aligned}
 A^T = & \Re \left[ (f_A - \eta g_E) g_M^* (\mathbf{p}' \cdot \mathbf{S}) - 2\eta g_M g_E^* (\mathbf{k}' \cdot \mathbf{S}) + 2r^2 \left( \frac{\eta g_E - f_A + 2\tau f_P}{\tau + r^2} ((\mathbf{p}' \cdot \mathbf{S}) \right. \right. \\
 & \left. \left. + (\mathbf{k}' \cdot \mathbf{S})) - f_P (\mathbf{p}' \cdot \mathbf{S}) \right) g_M^* - 2 \frac{1 + \tau}{\tau + r^2} (\tau f_A^3 + 2r^2 f_{P5}) f_A^* ((\mathbf{p}' \cdot \mathbf{S}) + (\mathbf{k}' \cdot \mathbf{S})) \right. \\
 & \left. + ((1 + \tau) f_A^3 + 2r^2 f_{P5}) f_A^* (\mathbf{p}' \cdot \mathbf{S}) + \eta f_A^3 g_E^* (\mathbf{p}' \cdot \mathbf{S}) + \eta r^2 \left( \frac{2(g_E - 2\eta f_A + r^2 f_T) - r^2 f_3}{\tau + r^2} \right. \right. \\
 & \left. \left. ((\mathbf{p}' \cdot \mathbf{S}) + (\mathbf{k}' \cdot \mathbf{S})) + \left( f_A^3 - \frac{f_3}{2} \right) (\mathbf{p}' \cdot \mathbf{S}) \right) f_T^* - \eta r^2 (1 + \tau) f_{P5} f_3^* (\mathbf{k}' \cdot \mathbf{S}) \right. \\
 & \left. - r^2 \left( \frac{\tau - r^2}{\tau + r^2} (\mathbf{p}' \cdot \mathbf{S}) + \frac{2\tau (\mathbf{k}' \cdot \mathbf{S})}{\tau + r^2} \right) (\eta g_M + f_A - 2f_P) f_T^* - \eta r^2 \left( (1 + \tau) f_{P5} + \frac{r^2 g_M}{\tau + r^2} \right. \right. \\
 & \left. \left. f_3^* ((\mathbf{p}' \cdot \mathbf{S}) + (\mathbf{k}' \cdot \mathbf{S})) \right) \right] - \frac{\rho_{\perp}}{\tau + r^2} \Im \left[ 2r^2 (g_M f_{P5}^* - f_A f_P^*) + \eta f_A g_E^* - \tau f_A^3 g_M^* \right. \\
 & \left. + r^2 (\eta f_A + f_A^3 + g_M - 2f_{P5}) f_T^* \right] + \eta r^2 \Re \left[ (4\eta f_P + r^2 f_3) f_{P5}^* - \frac{1}{2} g_M f_3^* \right] (\mathbf{p}' \cdot \mathbf{S}) \\
 & - \rho_{\perp} \eta r^2 \Im \left[ \left( f_P - \frac{1}{2} \frac{f_A}{\tau + r^2} \right) f_3^* \right],
 \end{aligned}$$

where  $\rho_{\perp} = \frac{\epsilon^{\mu\nu\lambda\rho} k_{\mu} k'_{\nu} p_{\lambda} S_{\rho}}{M^3} = 2\sqrt{\tau\nu^2 - (1 + \tau)(\tau + r^2)^2} \cos\phi_{\perp}$ .

# Current Constraints on Various Amplitudes

- ▶ Best constraint for  $\Re cf_{P5}$  comes from precise measurements of the beta decay rates. [J. C. Hardy and I. S. Towner, 2009]

$$\Re cf_{P5}(0)/f_1^V(0) = 0.0 \pm 1.8$$

- ▶  $\Im mf_{P5}$  is constrained by triple-correlation coefficient in the neutron decay. [A. Kozela et al., 2012]

$$\Im mf_{P5}(0) = -13 \pm 54$$

- ▶  $f_T$  and  $\Im mf_A$  are constrained from the fit to beta decay data. [M. González-Alonso et al., 2019, N. Severijns et al., 2006]

$$\Re cf_T(0) = -7.2 \pm 8.0$$

$$\Im mf_T(0) = 1.4 \pm 11.9$$

$$\Im mf_A(0) = 0.00034 \pm 0.00058$$

- ▶ For  $\Re cf_A^3$ , we have the following constraint. [M. Day and K. S. McFarland, 2012]

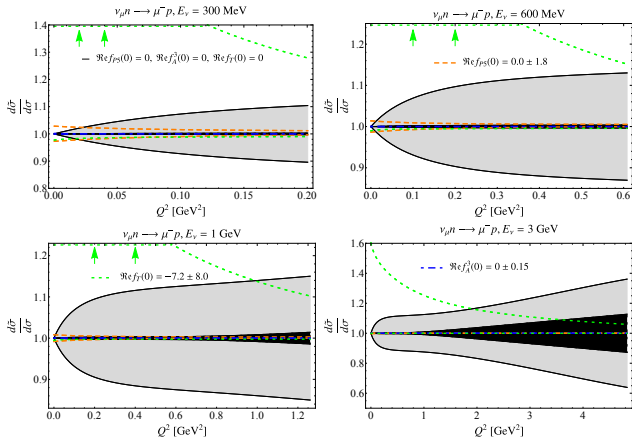
$$|\Re cf_A^3(0)| < 0.15$$

- ▶ For numerical estimates, we consider only either the real or the imaginary part of one additional amplitude at a time, assuming dipole form for  $Q^2$  dependence with  $\Lambda = 1$  GeV.

$$f_i^j(\nu, Q^2) = \frac{\Re cf_i^j(0) + i\Im mf_i^j(0)}{\left(1 + \frac{Q^2}{\Lambda^2}\right)^2}$$



# Unpolarized cross Section for Muon Neutrino



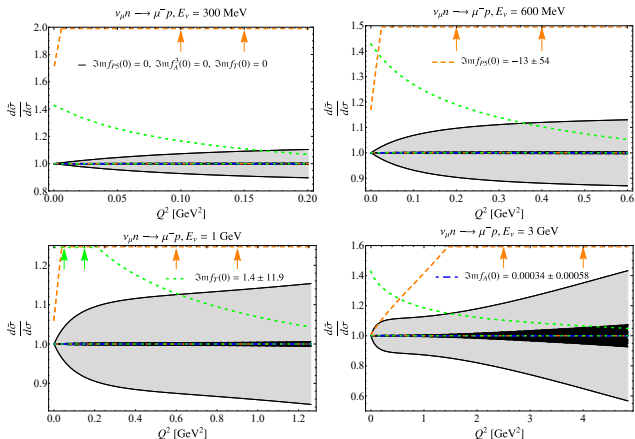
The ratio of the unpolarized cross section with one extra real-valued amplitude

$$f_i^j(\nu, Q^2) = \frac{\Re e f_i^j(0)}{\left(1 + \frac{Q^2}{\Lambda^2}\right)^2}, \text{ where } \Re e f_{P5}(0)/f_1^V(0) = -0.0 \pm 1.8, \Re e f_T(0) = -7.2 \pm 8.0,$$

$\Re e f_A^3(0) = 0 \pm 0.15$ , and  $\Lambda = 1 \text{ GeV}$ , to the tree-level result is shown as a function of the momentum transfer  $Q^2$  at various fixed muon neutrino energies. The **dark black band** corresponds to the **vector form-factor** uncertainty and the **light gray band** represents the uncertainty that comes from the **axial-vector form factor**.



# Unpolarized cross Section for Muon Neutrino

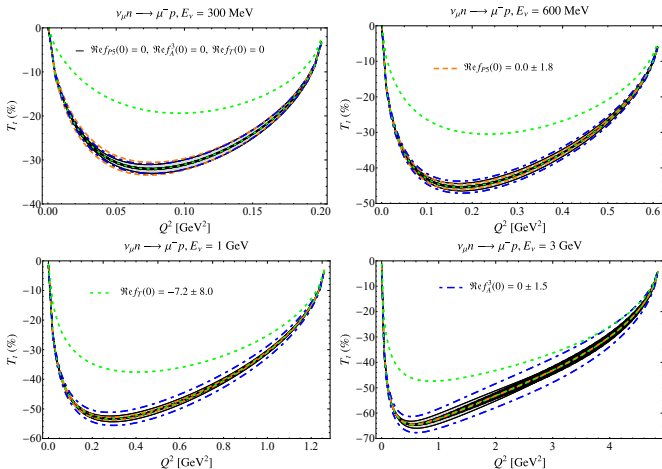


The ratio of the unpolarized cross section with one extra imaginary amplitude

$$f_i^j(\nu, Q^2) = \frac{i \Im m f_i^j(0)}{\left(1 + \frac{Q^2}{\Lambda^2}\right)^2}, \text{ where } \Im m f_{P5}(0)/f_1^V(0) = -13 \pm 54, \Im m f_T(0) = 1.4 \pm 11.9,$$

$\Im m f_A(0) = 0.00034 \pm 0.00058$ , and  $\Lambda = 1 \text{ GeV}$ , to the tree-level result is shown as a function of the momentum transfer  $Q^2$  at various fixed muon neutrino energies.

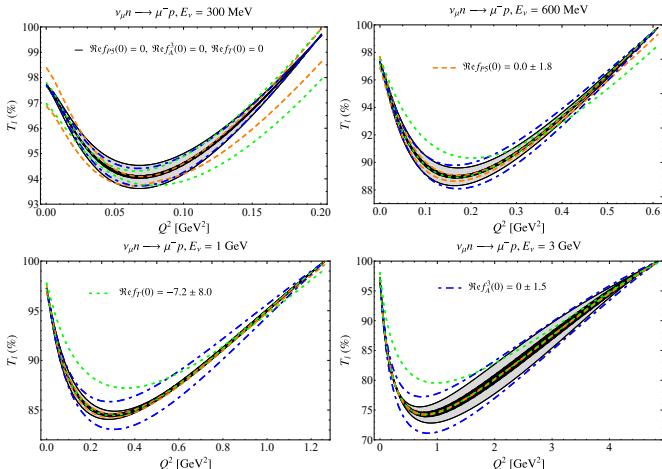
# Polarization Observable for Muon Neutrino, $T_t$



The **transverse polarization** observable  $T_t$ , target nucleon single-spin asymmetry, with one extra real-valued amplitude  $f_i^j(\nu, Q^2) = \frac{\Re e f_i^j(0)}{(1 + \frac{Q^2}{\Lambda^2})^2}$ , where  $\Re e f_{P5}(0)/f_1^V(0) = -0.0 \pm 1.8$ ,

$\Re e f_T(0) = -7.2 \pm 8.0$ ,  $\Re e f_\Lambda^3(0) = 0 \pm 0.15$ , and  $\Lambda = 1 \text{ GeV}$ , is compared to the tree-level result at various fixed muon neutrino energies.

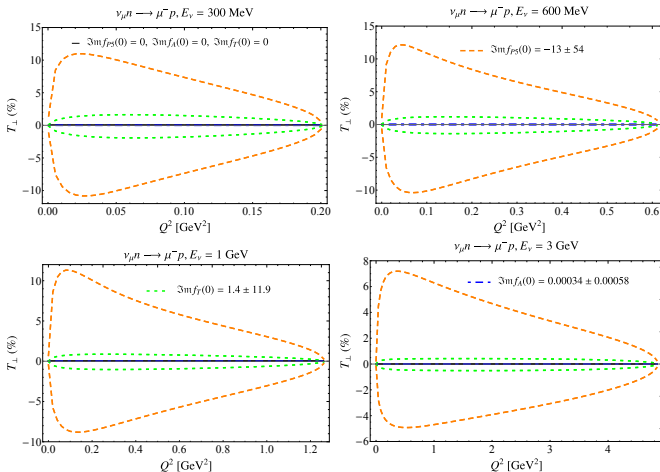
# Polarization Observable for Muon Neutrino, $T_l$



The longitudinal polarization observable  $T_l$ , target nucleon single-spin asymmetry, with one extra real-valued amplitude  $f_i^j(\nu, Q^2) = \frac{\Re \epsilon f_i^j(0)}{(1 + \frac{Q^2}{\Lambda^2})^2}$ , where  $\Re \epsilon f_{P5}(0)/f_1^V(0) = -0.0 \pm 1.8$ ,

$\Re \epsilon f_T(0) = -7.2 \pm 8.0$ ,  $\Re \epsilon f_A^3(0) = 0 \pm 0.15$ , and  $\Lambda = 1 \text{ GeV}$ , is compared to the tree-level result at various fixed muon neutrino energies.

# Polarization Observable for Muon Neutrino, $T_{\perp}$



The **transverse polarization** observable  $T_{\perp}$ , target nucleon single-spin asymmetry with **zero spin projection in the scattering plane**, with one extra imaginary amplitude

$$f_i^j(\nu, Q^2) = \frac{i \Im m f_i^j(0)}{\left(1 + \frac{Q^2}{\Lambda^2}\right)^2}, \text{ where } \Im m f_{P5}(0)/f_1^V(0) = -13 \pm 54, \Im m f_T(0) = 1.4 \pm 11.9,$$

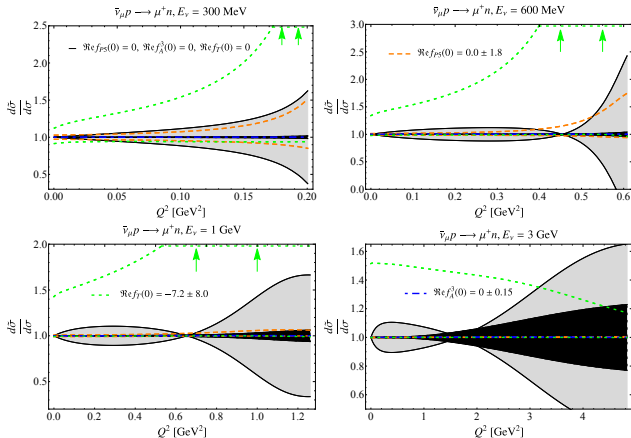
$\Im m f_A(0) = 0.00034 \pm 0.00058$ , and  $\Lambda = 1 \text{ GeV}$ , is compared to the tree-level result at various fixed muon neutrino energies.

# Conclusion

- ▶ Expressions for the **unpolarized cross section** and **single-spin asymmetries** in terms of (anti)neutrino-nucleon charged-current elastic scattering amplitudes are calculated **under a general framework**.
- ▶ Numerical results for **all observables** are plotted as a function of  $Q^2$  at relevant **fixed neutrino energies** with tree-level nucleon form factors.
- ▶ **QED contributions** to **unpolarized** muon (anti)neutrino-nucleon charged-current elastic scattering cross sections are **of the order of** the theoretical uncertainty, and **negligible** for **single-spin asymmetries**.
- ▶ Assuming **only dipole form** for  $Q^2$  dependence, for possible new physics contributions to the **invariant amplitudes**, the influence of **beta decay constraints** on **unpolarized cross sections** and **polarization observables** is estimated.
- ▶ The available constraints on both **real** and **imaginary** parts of the **tensor amplitude** as well as constraints on the **imaginary** part of the **scalar amplitude** can be significantly improved with current data on the **unpolarized antineutrino-hydrogen** and **neutrino-deuterium** cross sections.

# Backup Slides

# Unpolarized cross Section for Muon Antineutrino



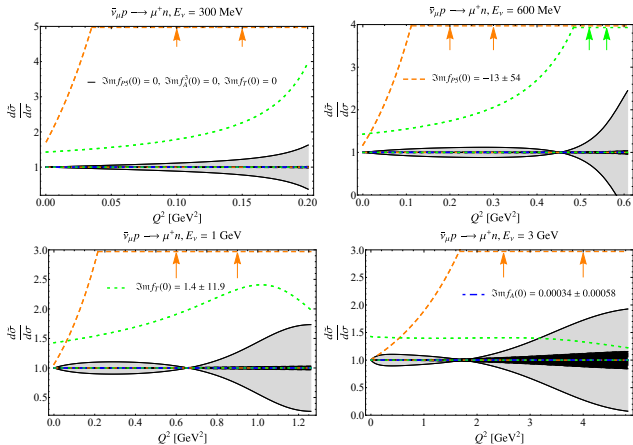
The ratio of the unpolarized cross section with one extra real-valued amplitude

$$f_i^j(\nu, Q^2) = \frac{\Re e f_i^j(0)}{\left(1 + \frac{Q^2}{\Lambda^2}\right)^2}, \text{ where } \Re e f_{P5}(0)/f_1^V(0) = -0.0 \pm 1.8, \Re e f_T(0) = -7.2 \pm 8.0,$$

$\Re e f_A^3(0) = 0 \pm 0.15$ , and  $\Lambda = 1 \text{ GeV}$ , to the tree-level result is shown as a function of the momentum transfer  $Q^2$  at various fixed muon neutrino energies. The dark black band corresponds to the vector form-factor uncertainty and the light gray band represents the uncertainty that comes from the axial-vector form factor.



# Unpolarized cross Section for Muon Antineutrino

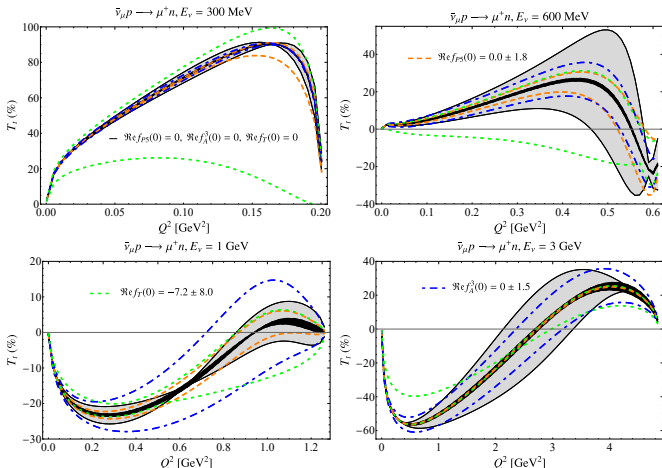


The ratio of the unpolarized cross section with one extra imaginary amplitude

$$f_i^j(\nu, Q^2) = \frac{i \Im m f_i^j(0)}{\left(1 + \frac{Q^2}{\Lambda^2}\right)^2}, \text{ where } \Im m f_{P5}(0)/f_1^V(0) = -13 \pm 54, \Im m f_T(0) = 1.4 \pm 11.9,$$

$\Im m f_A(0) = 0.00034 \pm 0.00058$ , and  $\Lambda = 1$  GeV, to the tree-level result is shown as a function of the momentum transfer  $Q^2$  at various fixed muon neutrino energies. The dark black band corresponds to the vector form-factor uncertainty and the light gray band represents the uncertainty that comes from the axial-vector form factor.

# Polarization Observable for Muon Antineutrino, $T_t$

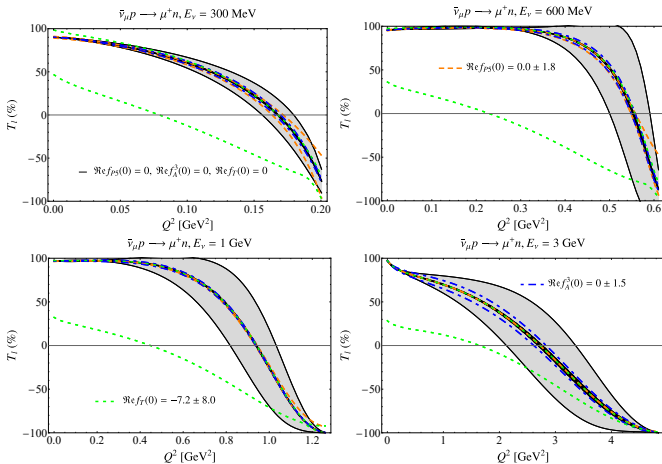


The transverse polarization observable  $T_t$ , target nucleon single-spin asymmetry, with one

extra real-valued amplitude  $f_i^j(\nu, Q^2) = \frac{\Re e f_i^j(0)}{(1 + \frac{Q^2}{\Lambda^2})^2}$ , where  $\Re e f_{P5}(0)/f_1^V(0) = -0.0 \pm 1.8$ ,

$\Re e f_T(0) = -7.2 \pm 8.0$ ,  $\Re e f_A^3(0) = 0 \pm 0.15$ , and  $\Lambda = 1 \text{ GeV}$ , is compared to the tree-level result at various fixed muon neutrino energies.

# Polarization Observable for Muon Antineutrino, $T_l$

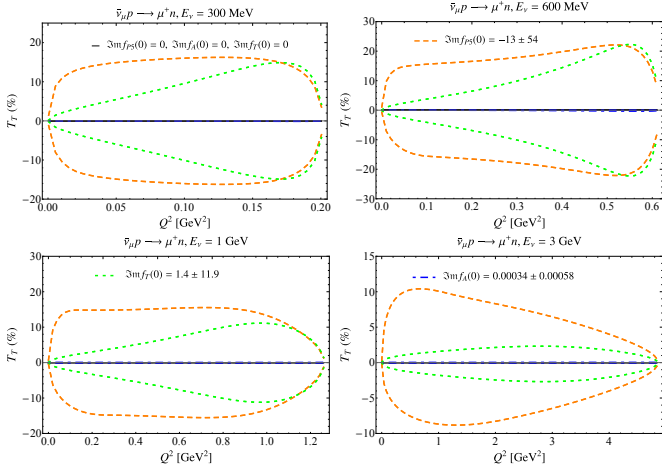


The longitudinal polarization observable  $T_l$ , target nucleon single-spin asymmetry, with one

extra real-valued amplitude  $f_i^j(\nu, Q^2) = \frac{\Re \epsilon f_i^j(0)}{(1 + \frac{Q^2}{\Lambda^2})^2}$ , where  $\Re \epsilon f_{P5}(0)/f_1^V(0) = -0.0 \pm 1.8$ ,

$\Re \epsilon f_T(0) = -7.2 \pm 8.0$ ,  $\Re \epsilon f_A^3(0) = 0 \pm 0.15$ , and  $\Lambda = 1 \text{ GeV}$ , is compared to the tree-level result at various fixed muon neutrino energies.

# Polarization Observable for Muon Antineutrino, $T_{\perp}$

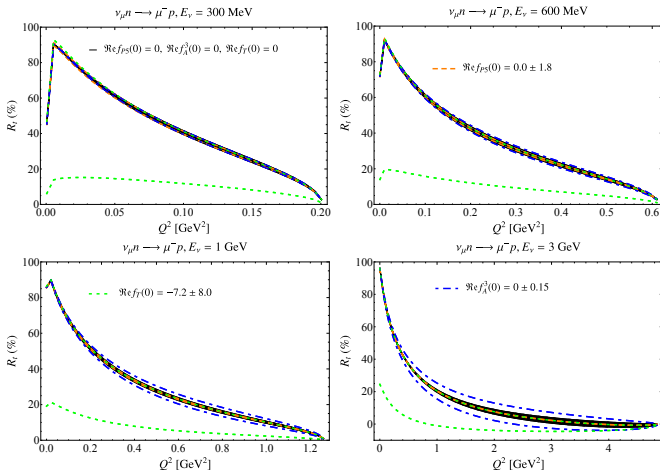


The transverse polarization observable  $T_{\perp}$ , target nucleon single-spin asymmetry with zero spin projection in the scattering plane, with one extra imaginary amplitude

$$f_i^j(\nu, Q^2) = \frac{i \Im m f_i^j(0)}{\left(1 + \frac{Q^2}{\Lambda^2}\right)^2}, \text{ where } \Im m f_{P5}(0)/f_1^V(0) = -13 \pm 54, \Im m f_T(0) = 1.4 \pm 11.9,$$

$\Im m f_A(0) = 0.00034 \pm 0.00058$ , and  $\Lambda = 1$  GeV, is compared to the tree-level result at various fixed muon neutrino energies.

# Polarization Observable for Muon Neutrino, $R_t$

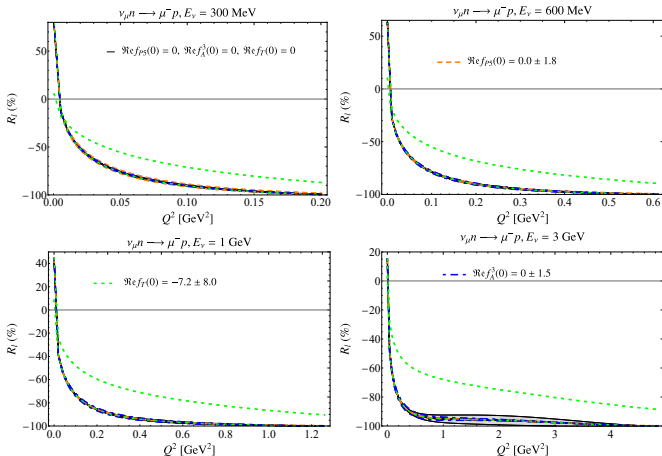


The transverse polarization observable  $R_t$ , recoil nucleon single-spin asymmetry, with one

extra real-valued amplitude  $f_i^j(\nu, Q^2) = \frac{\Re \epsilon f_i^j(0)}{(1 + \frac{Q^2}{\Lambda^2})^2}$ , where  $\Re \epsilon f_{p5}(0)/f_1^V(0) = -0.0 \pm 1.8$ ,

$\Re \epsilon f_T(0) = -7.2 \pm 8.0$ ,  $\Re \epsilon f_A^3(0) = 0 \pm 0.15$ , and  $\Lambda = 1 \text{ GeV}$ , is compared to the tree-level result at various fixed muon neutrino energies.

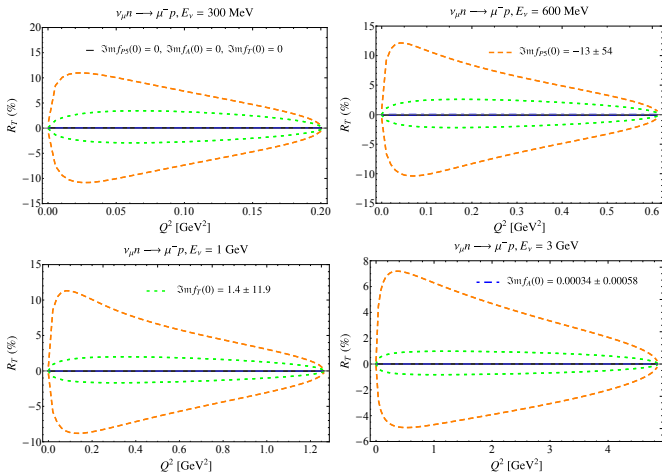
# Polarization Observable for Muon Neutrino, $R_L$



The longitudinal polarization observable  $R_L$ , recoil nucleon single-spin asymmetry, with one extra real-valued amplitude  $f_i^j(\nu, Q^2) = \frac{\Re \epsilon f_i^j(0)}{\left(1 + \frac{Q^2}{\Lambda^2}\right)^2}$ , where  $\Re \epsilon f_{P5}(0)/f_1^V(0) = -0.0 \pm 1.8$ ,

$\Re \epsilon f_T(0) = -7.2 \pm 8.0$ ,  $\Re \epsilon f_A^3(0) = 0 \pm 0.15$ , and  $\Lambda = 1 \text{ GeV}$ , is compared to the tree-level result at various fixed muon neutrino energies.

# Polarization Observable for Muon Neutrino, $R_{\perp}$

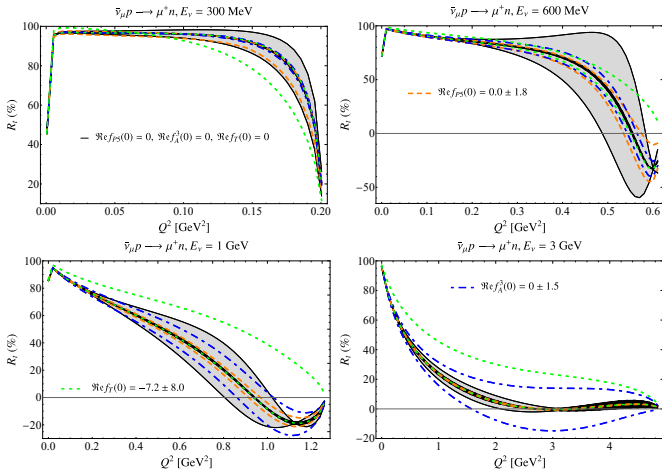


The transverse polarization observable  $R_{\perp}$ , recoil nucleon single-spin asymmetry with zero spin projection in the scattering plane, with one extra imaginary amplitude

$$f_1^j(\nu, Q^2) = \frac{i \Im m f_1^j(0)}{\left(1 + \frac{Q^2}{\Lambda^2}\right)^2}, \text{ where } \Im m f_{P5}(0)/f_1^V(0) = -13 \pm 54, \Im m f_T(0) = 1.4 \pm 11.9,$$

$\Im m f_A(0) = 0.00034 \pm 0.00058$ , and  $\Lambda = 1 \text{ GeV}$ , is compared to the tree-level result at various fixed muon neutrino energies.

# Polarization Observable for Muon Antineutrino, $R_t$



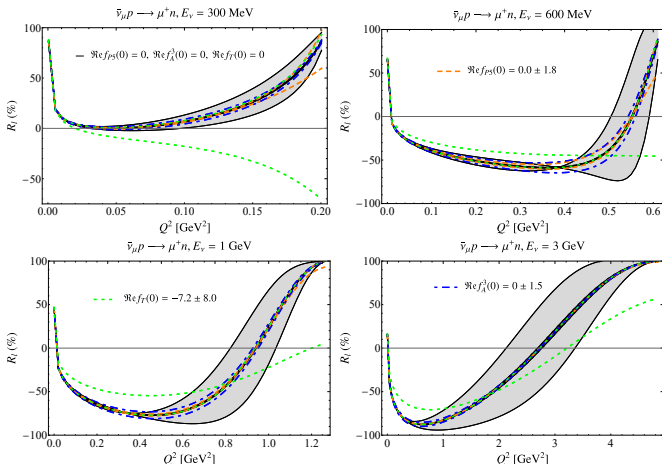
The transverse polarization observable  $R_t$ , recoil nucleon single-spin asymmetry, with one

extra real-valued amplitude  $f_i^j(\nu, Q^2) = \frac{\Re e f_i^j(0)}{(1 + \frac{Q^2}{\Lambda^2})^2}$ , where  $\Re e f_{P5}(0)/f_1^V(0) = -0.0 \pm 1.8$ ,

$\Re e f_T(0) = -7.2 \pm 8.0$ ,  $\Re e f_A^3(0) = 0 \pm 0.15$ , and  $\Lambda = 1 \text{ GeV}$ , is compared to the tree-level result at various fixed muon neutrino energies.



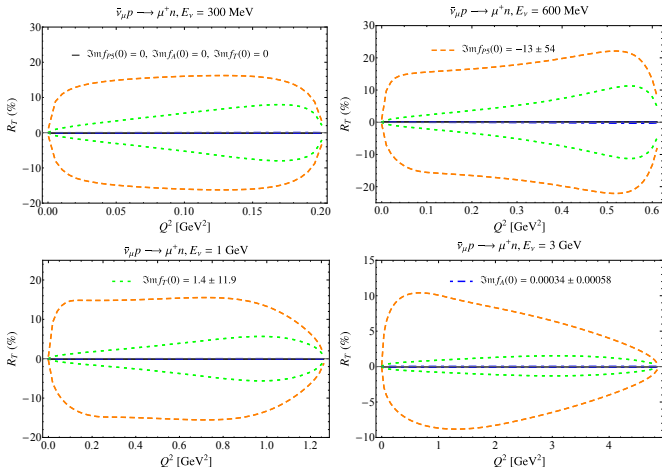
# Polarization Observable for Muon Antineutrino, $R_t$



The longitudinal polarization observable  $R_t$ , recoil nucleon single-spin asymmetry, with one extra real-valued amplitude  $f_i^j(\nu, Q^2) = \frac{\Re e f_i^j(0)}{(1 + \frac{Q^2}{\Lambda^2})^2}$ , where  $\Re e f_{P5}(0)/f_1^V(0) = -0.0 \pm 1.8$ ,

$\Re e f_T(0) = -7.2 \pm 8.0$ ,  $\Re e f_A^3(0) = 0 \pm 0.15$ , and  $\Lambda = 1 \text{ GeV}$ , is compared to the tree-level result at various fixed muon neutrino energies.

# Polarization Observable for Muon Antineutrino, $R_{\perp}$

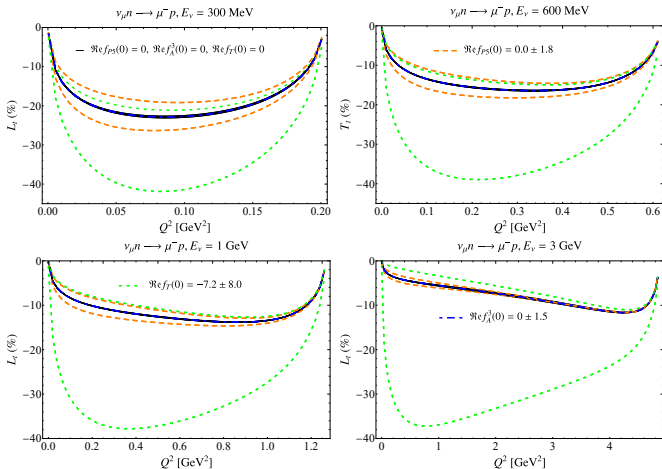


The transverse polarization observable  $R_{\perp}$ , recoil nucleon single-spin asymmetry with zero spin projection in the scattering plane, with one extra imaginary amplitude

$$f_i^j(\nu, Q^2) = \frac{i \Im m f_i^j(0)}{\left(1 + \frac{Q^2}{\Lambda^2}\right)^2}, \text{ where } \Im m f_{P5}(0)/f_1^V(0) = -13 \pm 54, \Im m f_T(0) = 1.4 \pm 11.9,$$

$\Im m f_A(0) = 0.00034 \pm 0.00058$ , and  $\Lambda = 1 \text{ GeV}$ , is compared to the tree-level result at various fixed muon neutrino energies.

# Polarization Observable for Muon Neutrino, $L_t$

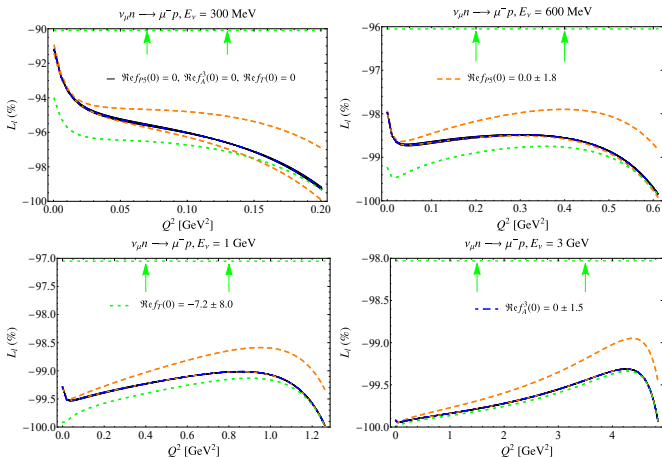


The transverse polarization observable  $L_t$ , recoil lepton single-spin asymmetry, with one extra

real-valued amplitude  $f_i^j(\nu, Q^2) = \frac{\Re \epsilon f_i^j(0)}{(1 + \frac{Q^2}{\Lambda^2})^2}$ , where  $\Re \epsilon f_{P5}(0)/f_1^V(0) = -0.0 \pm 1.8$ ,

$\Re \epsilon f_T(0) = -7.2 \pm 8.0$ ,  $\Re \epsilon f_A^3(0) = 0 \pm 0.15$ , and  $\Lambda = 1$  GeV, is compared to the tree-level result at various fixed muon neutrino energies.

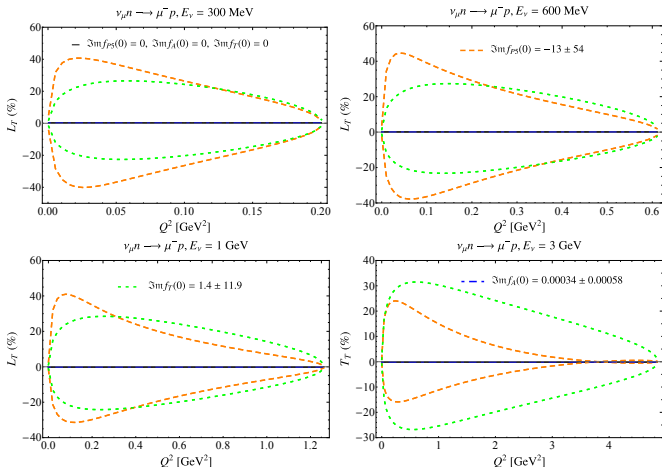
# Polarization Observable for Muon Neutrino, $L_t$



The longitudinal polarization observable  $L_t$ , recoil lepton single-spin asymmetry, with one extra real-valued amplitude  $f_i^j(\nu, Q^2) = \frac{\Re \epsilon f_i^j(0)}{(1 + \frac{Q^2}{\Lambda^2})^2}$ , where  $\Re \epsilon f_{P5}(0)/f_1^V(0) = -0.0 \pm 1.8$ ,

$\Re \epsilon f_T(0) = -7.2 \pm 8.0$ ,  $\Re \epsilon f_A^3(0) = 0 \pm 0.15$ , and  $\Lambda = 1 \text{ GeV}$ , is compared to the tree-level result at various fixed muon neutrino energies.

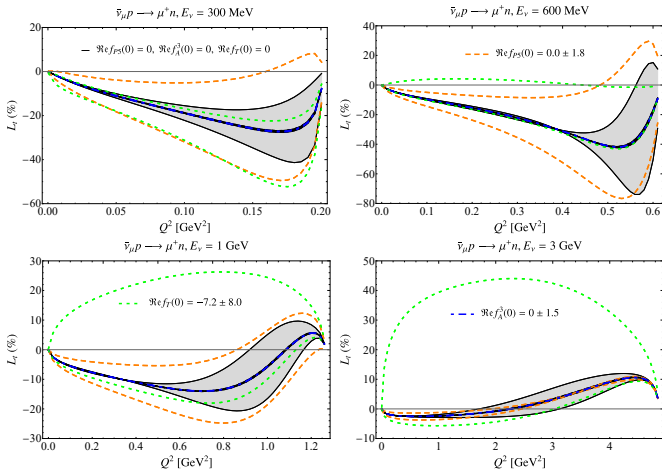
# Polarization Observable for Muon Neutrino, $L_{\perp}$



The transverse polarization observable  $L_{\perp}$ , recoil lepton single-spin asymmetry with zero spin projection in the scattering plane, with one extra imaginary amplitude  $f_i^j(\nu, Q^2) = \frac{i\Im m f_i^j(0)}{(1 + \frac{Q^2}{\Lambda^2})^2}$ ,

where  $\Im m f_{P5}(0)/f_1^V(0) = -13 \pm 54$ ,  $\Im m f_T(0) = 1.4 \pm 11.9$ ,  $\Im m f_A(0) = 0.00034 \pm 0.00058$ , and  $\Lambda = 1 \text{ GeV}$ , is compared to the tree-level result at various fixed muon neutrino energies,

# Polarization Observable for Muon Antineutrino, $L_t$

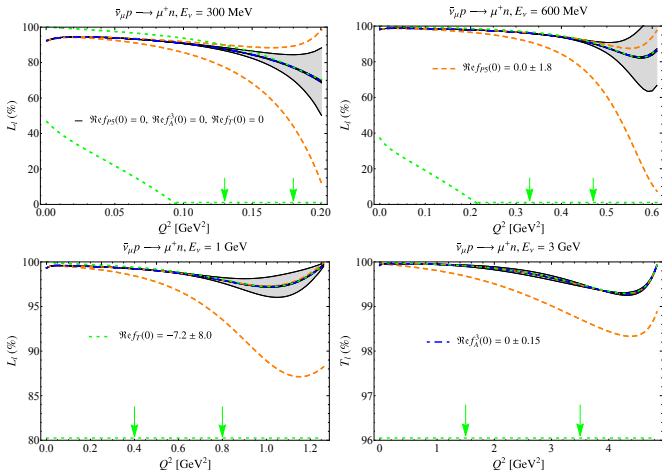


The transverse polarization observable  $L_t$ , recoil lepton single-spin asymmetry, with one extra

real-valued amplitude  $f_i^j(\nu, Q^2) = \frac{\Re e f_i^j(0)}{\left(1 + \frac{Q^2}{\Lambda^2}\right)^2}$ , where  $\Re e f_{P5}(0)/f_1^V(0) = -0.0 \pm 1.8$ ,

$\Re e f_T(0) = -7.2 \pm 8.0$ ,  $\Re e f_A^3(0) = 0 \pm 0.15$ , and  $\Lambda = 1 \text{ GeV}$ , is compared to the tree-level result at various fixed muon neutrino energies.

# Polarization Observable for Muon Antineutrino, $L_l$

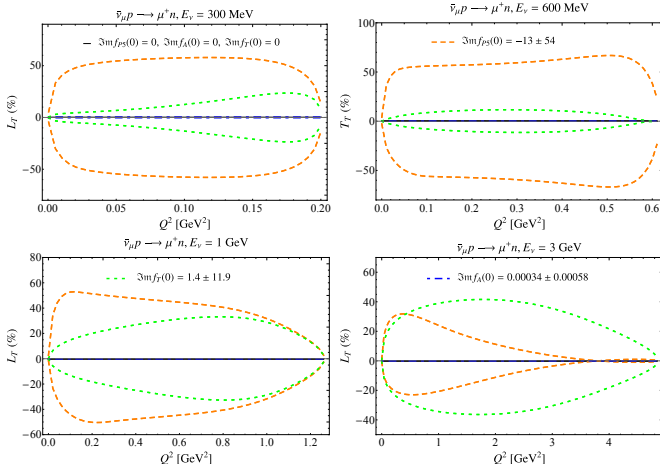


The longitudinal polarization observable  $L_t$ , recoil lepton single-spin asymmetry, with one

extra real-valued amplitude  $f_i^j(\nu, Q^2) = \frac{\Re \epsilon f_i^j(0)}{(1 + \frac{Q^2}{\Lambda^2})^2}$ , where  $\Re \epsilon f_{P5}(0)/f_1^V(0) = -0.0 \pm 1.8$ ,

$\Re \epsilon f_T(0) = -7.2 \pm 8.0$ ,  $\Re \epsilon f_A^3(0) = 0 \pm 0.15$ , and  $\Lambda = 1$  GeV, is compared to the tree-level result at various fixed muon neutrino energies.

# Polarization Observable for Muon Antineutrino, $L_{\perp}$



The transverse polarization observable  $L_{\perp}$ , recoil lepton single-spin asymmetry with zero spin projection in the scattering plane, with one extra imaginary amplitude  $f_i^j(\nu, Q^2) = \frac{i\Im m f_i^j(0)}{(1 + \frac{Q^2}{\Lambda^2})^2}$ ,

where  $\Im m f_{PS}(0)/f_1^V(0) = -13 \pm 54$ ,  $\Im m f_T(0) = 1.4 \pm 11.9$ ,  $\Im m f_A(0) = 0.00034 \pm 0.00058$ , and  $\Lambda = 1$  GeV, is compared to the tree-level result at various fixed muon neutrino energies,